The Spine Journal 19 (2019) 905–919

Basic Science

Safety of intradiscal delivery of triamcinolone acetonide by a poly(esteramide) microsphere platform in a large animal model of intervertebral disc degeneration

Imke Rudnik-Jansen, MS[a], Anna Tellegen, MS, DVM[b], Martijn Beukers, MS, DVM[b], Fetullah Öner, MS, PhD.[a], Nina Woike, MS[c], George Mihov, PhD.[c], Jens Thies, PhD.[c], Björn Meij, DVM, PhD.[b], Marianna Tryfonidou, DVM, PhD.[b], Laura Creemers, PhD.[a,*]

[a] *Department of Orthopaedics, University Medical Center Utrecht, HP G05.228, Postbus 85500, Heidelberglaan 100, 3508GA Utrecht, The Netherlands*

[b] *Department of Clinical Sciences of Companion Animals, Yalelaan 108, 3584 CM Utrecht, The Netherlands*

[c] *DSM Biomedical B.V., Koestraat 1, 6167 RA Geleen, The Netherlands*

Received 19 July 2018; revised 23 October 2018; accepted 23 October 2018

Abstract

BACKGROUND CONTEXT: Local corticosteroids have been used to relieve symptoms of chronic low back pain, although treatment effects have been shown to wear off relatively fast. Prolonging corticosteroid presence by controlled release from biomaterials may allow for longer pain relief while circumventing adverse effects such as high bolus dosages.

PURPOSE: The purpose of this study was to evaluate the safety and efficacy of intradiscal controlled release of triamcinolone acetonide (TAA) by poly(esteramide) microspheres in a canine degenerated intervertebral disc (IVD) model.

STUDY DESIGN: In a preclinical experimental large animal model, the effect of prolonged glucocorticoid exposure on disc degeneration was evaluated.

METHODS: Degeneration was accelerated by nucleotomy of lumbar IVDs of Beagle dogs. After 4 weeks, microspheres loaded with 8.4 μg TAA, and 0.84 mg TAA were administered to the degenerated IVDs by intradiscal injection (n=6 per group). Empty microspheres (n=6) and all adjacent non-nucleotomized noninjected IVDs were included as controls (n=24). Immediately prior to TAA administration and after 12 weeks, magnetic resonance imaging was performed. Degenerative changes were evaluated by disc height index, Pfirrmann grading, T1ρ and T2 mapping values, postmortem CT scans, macroscopic and microscopic grading, and biochemical/immunohistochemical analysis of inflammation and extracellular matrix content. In addition, nerve growth factor (NGF) protein expression, a biomarker for pain, was scored in nucleus pulposus (NP) tissues. The study was funded by a research grant from Health Holland (1.3 million euros = 1.5 million US dollars).

RESULTS: Macroscopic evaluation and CT images postmortem were consistent with mild disc degeneration. Other abnormalities were not observed. Nucleotomy-induced degeneration and inflammation was mild, reflected by moderate Pfirrmann grades and PGE_2 levels. Regardless of TAA dosage, local sustained delivery did not affect disc height index nor Pfirrmann grading, T1ρ and T2 mapping values, PGE_2 tissue levels, collagen, GAG, and DNA content. However, the low dosage of TAA microspheres significantly reduced NGF immunopositivity in degenerated NP tissue.

FDA device/drug status: Not approved for this indication (triamcinolone acetonide in polyesteramide microspheres); Investigational (poly(esteramide) microspheres).

Author disclosures: ***IRJ:*** Grants: LSH/Health Holland (F, paid directly to institution; D, salary). ***AT:*** Grants: LSH/Health Holland (F, paid directly to institution; D, salary). ***MB:*** Grant: LSH/Health Holland (F, paid directly to institution). ***FO:*** Grant: LSH/Health Holland (F, paid directly to institution). ***NW:*** Nothing to disclose. ***GM:*** Nothing to disclose. ***JT:*** Nothing to disclose. ***BM:*** Grant: LSH/Health Holland (F, paid directly to institution). ***MT:*** Grant: LSH/Health Holland (F, paid directly to institution). ***LC:*** Grant: LSH/Health Holland (F, paid directly to institution).

* Corresponding author. Department of Orthopaedics, University Medical Center Utrecht, HP G05.228, Postbus 85500, Heidelberglaan 100, 3508GA Utrecht, The Netherlands. Tel.: (+31)088-7550293.

E-mail address: l.b.creemers@umcutrecht.nl (L. Creemers).

https://doi.org/10.1016/j.spinee.2018.10.014

CONCLUSIONS: This is the first in vivo application in a preclinical large animal model of a controlled release formulation of corticosteroids in mild IVD degeneration. Sustained release of TAA locally in the IVD appeared safe and reduced NGF expression, suggesting its potential applicability for pain relief, although beneficial effects were absent on tissue degeneration.
CLINICAL SIGNIFICANCE: The present platform seems to be promising in extending the local controlled delivery of TAA with the potency to provide long-standing analgesia in the subset of LBP patients suffering from discogenic pain.

Keywords: chronic low back pain; intradiscal injection; controlled release; corticosteroid; triamcinolone acetonide; intervertebral disc degeneration; poly(esteramide) microspheres; preclinical animal model.

Introduction

Chronic low back pain (LBP), affecting millions of people worldwide, is strongly associated with intervertebral disc (IVD) degeneration [1]. It is one of the most common causes of disability and imparts a huge socioeconomic burden, mostly due to decreased productivity [2]. Since population age and associated risk factors for IVD degeneration are increasing, prevalence is increasing [3]. During degeneration, the structural organization of the nucleus pulposus (NP) and annulus fibrosus (AF) are subjected to several morphologic and molecular changes; extracellular matrix (ECM) proteins are lost from the framework, in particular PGs [4,5] changing disc homeostasis toward a more catabolic environment. Subsequently, water content also decreases in the disc tissue leading to a disorganized ECM and eventually a loss of disc height [5,6]. This finally results in a disorder of the spine motion segment due to reduced ability of the IVD to absorb shocks. The loss of IVD tissue integrity can also contribute to increased instability of the spinal segment, a potential risk factor for LBP and possible complications like degenerative slip and stenosis [7]. Pain is the predominant clinical symptom and even though the mechanism is in most cases unknown, it is often attributed to anatomical pain generators such as the IVD or the facet joint [8]. Although there is considerable debate on the origin of the discogenic pain signal in the degenerated IVD, it is speculated that a degenerating IVD becomes painful due to the secretion of growth factors such as nerve growth factor (NGF) that can stimulate peripheral nociceptive sensory neurons to grow into the IVD [9–11].

Inflammation-induced LBP is commonly treated using anti-inflammatory agents, such as corticosteroids or nonsteroidal drugs, which are administered orally or by local injection [12,13]. Although corticosteroids are widely used for their strong potency to reduce inflammation, concerns for their long-term use arise for adverse side effects such as glucocorticoid-induced osteoporosis [14–16]. Administration via intradiscal injection can reduce the risk of systemic side effects and could be a good alternative therapy delaying more invasive treatment options such as surgery [17]. However, the effectiveness of intradiscal steroid injections has been subject of debate, and contradicting treatment outcomes in terms of pain relief have been reported [18–21]. Clinical trials showed a temporary or no effect at all [18,19,22,23]. Most of the trials showing an absence of effects were based on intradiscal injection of Depo-Medrol, a formulation of methylprednisolone acetate that has shown to induce degeneration and matrix calcification in rabbit IVDs through the polyethylene glycol (PEG)-containing vehicle suspension [24]. Methylprednisolone succinate injected in a sodium phosphate buffer without PEG did not induce these effects, suggesting not only the safety of corticosteroids but also the importance of the delivery vehicle used. This is further corroborated by the fact that upon intrathecal and epidural administration, PEG-based formulations were shown to be toxic [25]. Other vehicle excipients used in steroid formulations, such as benzyl alcohol or carboxymethylcellulose, were toxic in ocular tissues upon intravitreal injection [26]. Also, ossification and calcification in the spinal canal have been reported after intradiscal steroid injections that were likely attributable to the excipients, although no vehicle controls were included [20,27]. Clinical trials on intradiscal application of other formulations of corticosteroids did show pain relief, although generally the effect did not last longer than 1 to 6 months, most likely due to relatively rapid loss of the drug to the circulation [17,22]. Hence, therapeutic drug delivery approaches allowing for safe and prolonged exposure to corticosteroids may be more appropriate to provide long-term pain reduction.

In small animals, safety of intradiscal application of corticosteroids in ceramic capsules or poly(lactic-co-glycolic acid) (PLGA) microparticles was shown at histologic level in rat models of induced tail IVD degeneration [28,29]. However, rat tail IVD sizes and volumes pose a challenge in the translation of novel treatments to human application, and tail IVDs are comparable to human lumbar IVDs only to a very limited extent [30]. Since the IVD degeneration process in dogs is similar to that in humans, this represents a clinically relevant animal model for human IVD degeneration [31]. The safety of intradiscal injection of several biomaterials [32,33] including a novel biomaterial platform consisting of poly(esteramide) microspheres (PEAMs) was already demonstrated in a canine model of spontaneous IVD degeneration [34]. PEAMs are mainly degraded via enzymatic degradation, contributing to the slow release of the incorporated corticosteroid [35]. Retention of PEAMs

in healthy and degenerated rat knee joints was shown to last up to 10 weeks after intra-articular injection, and when loaded with triamcinolone acetonide (TAA), inflammation was suppressed up to 11 weeks in osteoarthritic knee joints [36]. Whether TAA is also suitable as therapy in a joint with a confined space such as the IVD still has to be determined. To this end, we evaluated in a clinically relevant large animal model the safety and anti-inflammatory potency of prolonged exposure of TAA in two dosages on IVD tissues and adjacent spinal bone segments.

Material and methods

Synthesis and preparation of poly(esteramide) microspheres. PEA was synthesized according to previously described methods [34,37]. PEA polymer alone (for empty PEAMs) or loaded with 30 wt% TAA was dissolved in dichloromethane (Merck Millipore). The homogenized solution was sonicated in a water bath for 3 minutes. Then, PEA solution was emulsified in 20 mL of water phase, (poly(vinyl alcohol, Sigma-Aldrich, 1 wt% and NaCl 2.5 wt%) by the use of an ultraturrax, and stirred at 8,000 rpm for 3 minutes. After emulsification, particles were poured into a hardening bath of 100 mL water phase and were hardened overnight under airflow. Particles were cooled with an ice-bath for 1 hour and thereafter washed with 0.04% Tween 80 (Merck). Excessive surfactant was removed by centrifugation. Before freeze-drying to remove residual solvent, particles were suspended in 0.04% Tween 80 (Merck) in order to reach the right concentration of PEA particles per volume; empty PEA 70 mg/mL, PEA TAA low dosage 0.72 mg/mL, and PEA TAA high dosage 72 mg/mL particle concentration. Once dried, the particles were weighed in individual HPLC vials to the approximate amount of 30 to 35 mg and γ-sterilized on dry ice.

Surgical procedures. All animal procedures were approved and conducted in accordance with the guidelines set out by the Ethics Committee of Animal Experiments of Utrecht University (AVD# 108002015285). Six male Beagle dogs (Marshall) with a median age of 1.92 years (range 1.90–1.95) and median weight of 8.8 kg (range 8.0–9.6) underwent general clinical and orthopedic examination by a board-certified veterinary surgeon (BM) before entering the study. At the initiation of the study, dogs accommodated to their new environment for at least 1 week and were housed in groups.

Complying with the 3Rs principles, three Beagles were used to study the effects of sustained TAA release, the other three for a similar study on another small molecule drug. To reduce animal use, thoracic IVDs (T12–T13) of the six Beagles were injected with empty PEAMs and served as control for both studies. Adjacent non-nucleotomized discs (four per dog) of all six dogs were included in the analysis as healthy controls to serve as a baseline control, hereafter referred to as noninduced discs. Altogether, in the study, there were 24 noninduced untreated IVDs; 6 degenerated IVDs receiving empty PEAMs, 6 degenerated IVDs receiving PEAMs+TAA (low dosage, ld), and 6 degenerated IVDs receiving PEAMs+TAA (high dosage, hd).

Nucleotomy-induced degeneration. Beagle dogs spontaneously develop mild IVD degeneration [38]. To enhance the level of degeneration, in each dog, additional IVD degeneration was induced by removing part of the NP tissue in five alternating IVDs 4 weeks before treatment (t_{-4}) at level T12–T13, L1–L2, L3–L4, L5–L6, and L7–S1. Adjacent IVDs were included as non-nucleotomized controls. Overview of experimental setup is given in Table 1. All dogs received preoperative analgesia by IV administration of carprofen (4 mg/kg) and buprenorphine (20 μg/kg). Premedication consisted of IV dexmedetomidine (2 μg/kg/hr), followed by induction anesthesia consisting of 1 to 2 mg/kg IV propofol. Subsequently, animals received endotracheal tubes to deliver 1% to 1.5% vol/vol isoflurane gas for maintenance anesthesia during surgery, delivered in a 1:1 (oxygen:air) mixture. Continuous rate infusion of ketamine (10 μg/kg/min) and dexmedetomidine (2 μg/kg/hr) was administered by IV injection as perioperative analgesia. Heart rate, body temperature, respiration rate, carbon dioxide, and oxygen levels were monitored during the surgical (degeneration induction and PEAMs injection) and diagnostic imaging procedures. Dogs were positioned in a right recumbent position and surgery on the left lateral side was performed under aseptic conditions. After IVDs were localized, an 18G needle was inserted in the outer AF and correct needle placement was confirmed by intraoperative fluoroscopy. Lumbosacral discs were percutaneously approached, under fluoroscopic guidance. Subsequently, the needle was further inserted through the AF into the NP center, and a part of the NP was aspirated using a 10 mL syringe. Postoperatively, all animals received carprofen (subcutaneously, 4 mg/kg) and buprenorphine (intramuscularly, 20 μg/kg) as analgesia for 3 days. During the first postoperative week, dogs were monitored daily by a veterinarian (AT) and thereafter at least on a weekly basis.

Poly(esteramide) microsphere injection. Four weeks after nucleotomy-induced degeneration surgery, intradiscal injections were done by a board-certified veterinary surgeon (BM) under fluoroscopic guidance to confirm correct needle position prior to injection. PEAM injections were done using 100 μL gastight Hamilton syringes (7656-01 model 1710 RN, Hamilton Company USA) connected to 27G needles (25 mm, 12° beveled point, Hamilton Company USA). A total of 40 μL was injected slowly into each nucleotomized IVD on the contralateral (right) side with the same anesthesia protocol used for nucleotomy-induced degeneration. After injection, needle was kept in place a few seconds before retracting, to prevent leakage. Buprenorphine (intramuscularly, 20 μg/kg) was used as pre- and postoperative analgesia. Empty PEAMs (70 mg/mL particles) served as control and were injected into T12–T13 IVD, the remaining IVDs were injected with TAA-loaded PEAMs (low dosage ld; 0.72 mg/mL particles;

Table 1
Experimental design of in vivo Beagle IVD study

	Week	−4 (t_{-4})	0 (t_0)	12 (t_{12})	Postmortem
IVD degeneration induction		X			
PEAMs injection			X		
MRI;			X	X	
- DHI					
- Pfirrmann					
- T1ρ values					
- T2 values					
CT					X
Macroscopic evaluation					X
Microscopic evaluation					X
Biochemical assays					X

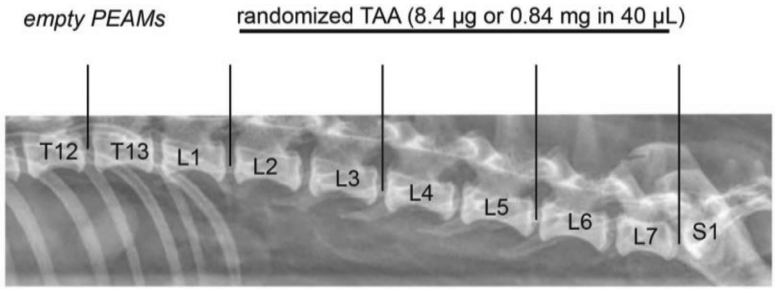

CT, computed tomography; DHI, disc height index; IVD, intervertebral disc; L, lumbar vertebrae; MRI, magnetic resonance imaging; PEAMs, polyesteramide microspheres; S, sacral vertebrae; T, thoracic vertebrae; TAA, triamcinolone acetonide.

8.4 μg TAA and high dosage hd; 72 mg/mL particles; 0.84 mg TAA) diluted in sterile saline. TAA-PEAM conditions were randomized with n=2 per dog. Overview of randomized experimental setup is given in Table 2.

Magnetic resonance imaging. Magnetic resonance images (MRI) were obtained pre- (t_0) and post-treatment (t_{12}) using a 1.5 Tesla system (Ingenia, Philips, Best, the Netherlands) under general anesthesia consisting of IV propofol (1−2 mg/kg). Before anesthesia induction, dogs received IV dexmedetomidine (10 μg/kg) and butorphanol (0.1 mg/kg) as premedication. Sagittal T2-weighted Turbo Spin Echo (repetition time [TR]=3,000, echo time [TE] =110 ms, acquisition matrix =124 × 261) and T1-weighted Turbo Spin Echo (TR=400 ms, TE=8 ms, acquisition matrix=124 × 313) images were acquired using a field of view of 75 × 220 mm and thirteen 2 mm thick slices. To measure T2 relaxation times, a quantitative multiple spin-echo T2-mapping sequence was used (scan parameters: FOV=75 × 219 mm, acquisition matrix=96 × 273, slice thickness=3 mm, TR=2,000, TE=13 ms to TE=104 ms with 13 ms echo spacing). A spin-lock-prepared sequence with a 3-dimensional multishot gradient echo (T1−TFE) readout was used for T1ρ-weighted imaging (scan parameters: FOV=76 × 220 mm, acquisition matrix=76 × 220 slice thickness=2 mm, TR/TE=4.6 s/2.3, TR=5 ms, TE=2.5 ms, TFE factor=50, flip angle=45°, shot interval=3,000 ms). Different spin-lock times of 0, 10, 20, 30, and 40 ms, with a spin-lock pulse amplitude set to 500 Hz, were used to allow for quantitative T1ρ mapping. Mid-sagittal slices of T2-weighted MR images were used to determine the IVD degeneration grade using Pfirrmann scoring [39] (MB/AT) and the disc height index (DHI) [34] (AT/IJ) of each IVD. Grading was done blinded to treatment location for both time points (t_0 and t_{12}). Analysis of quantitative MR images

Table 2
Overview of randomized conditions per IVD in each dog

	T12−T13	T13−L1	L1−L2	L2−L3	L3−L4	L4−L5	L5−L6	L6−L7	L7−S1
Dog 1	Empty PEAMs	n.i.	TAA ld	n.i.	TAA ld	n.i.	TAA hd	n.i.	TAA hd
Dog 2	Empty PEAMs	n.i.	TAA ld	n.i.	TAA hd	n.i.	TAA hd	n.i.	TAA ld
Dog 3	Empty PEAMs	n.i.	TAA hd	n.i.	TAA ld	n.i.	TAA hd	n.i.	TAA ld
Dog 4−6	Empty PEAMs	n.i.		n.i.		n.i.		n.i.	

L, lumbar vertebrae; ld, low dose; hd, high dose; n.i., not injected; PEAMs, polyesteramide microspheres; S, sacral vertebrae; T, thoracic vertebrae; TAA, triamcinolone acetonide.

Nucleotomy-induced degenerated discs: T12−T13, L1−L2, L3−L4, L5−L6, L7−S1.

by T1ρ and T2 mapping was done by voxel wise fitting and calculation of the mean signal intensity in each ROI of the NP, as previously published [34,40].

Postmortem computed tomography imaging and collection of spinal units. Twelve weeks after intradiscal PEAMs injection (t_{12}), dogs were euthanized by sedation with dexmedetomidine followed by IV pentobarbital (200 mg/kg). *Post-mortem*, computed tomography (CT) images were obtained of the whole vertebral column to evaluate bone structures. A third-generation 64-slice CT scanner (Siemens Somatom Definition AS, Siemens Healthcare, The Hague, the Netherlands) was used to obtain CT images (scan parameters: 0.6 mm slice thickness, 120 kV, 350 mAs, 1,000 ms tube rotation time, 0.35 spiral pitch factor, 512 × 512 pixel matrix and a fixed field of view of 93 mm). Transverse and sagittal reconstructions of 0.6 mm thick slices were made using soft tissue and bone reconstruction kernels. Nine spinal units (one-half vertebrae – IVD – one-half vertebrae) were harvested of each dog, and every unit was transected mid-sagittal, still containing both NP and AF tissues. One half was snap frozen in liquid nitrogen and stored at −80˚C for biomolecular and biochemical analysis. The other part was photographed (Olympus BX41, Hamburg, Germany) for macroscopic evaluation and fixed in 4% buffered formaldehyde solution (Klinipath, Duiven, the Netherlands) for 2 weeks at room temperature (RT). Macroscopic images of the halved IVD segments were evaluated in a blinded fashion in random order according to the Thompson grading scheme modified for dogs [41] by 2 investigators (AT/IR) independently.

Histopathologic scoring. After fixation, the IVD segments were decalcified in 0.5M EDTA for 9 weeks under continuous agitation. Every 2 weeks, tissues were refixed 4% buffered formaldehyde for 48 hours. The segments were dehydrated in ascending alcohol series 70%, 96%, 100%, and eventually in xylene and subsequently embedded in paraffin. Five micrometer tissue sections were stained with hematoxylin & eosin and picosirius red/alcian blue. Scoring of IVD degeneration by the Boos histopathologic grading system validated for canines [42] was performed in a random order by two investigators (AT/IR) independently, blinded for treatments.

Immunohistochemistry. Immunohistochemistry was performed on 5 μm paraffin sections. After deparaffinization and rehydration, sections were washed with PBS or TBS and subsequently blocked for nonspecific endogenous peroxidase for 10 minutes at RT and washed 2 times with PBS of TBS containing 0.1% Tween 20 (PBST/TBST) for 5 minutes. Protocol overview is shown in Table 3 for the respective antibodies. Antigen retrieval was performed for 30 minutes at 37˚C. After washing, sections were blocked for 30 minutes and incubated overnight at 4˚C with the primary antibody (collagen type I, II or X and NGF). The next day, sections were washed with PBST or TBST and incubated with the secondary antibody for 30 minutes at RT. After washing, sections were incubated with 3,3'-Diaminobenzidine (DAB) substrate for 10 minutes, counterstained with Mayer's hematoxylin for 1 minute and rinsed with running tap water for 10 minutes. Before permanent mounting with Depex (06522, Sigma-Aldrich), slides were dehydrated with series ethanol and eventually xylene. For quantification of NGF [43], of each NP section per microscope slide, six digital images were obtained and total cell count as well as NGF immunopositive cells were manually counted and averaged using Photoshop count tool (Adobe Photoshop CS6, version 12.0.1 × 64).

Biochemistry: DNA, collagen, glycosaminoglycans (GAGs). NP and AF tissue were separated during cryosectioning of the snap frozen spinal unit, based on anatomical location of the tissues and stored in Complete lysis M EDTA-free buffer (Roche Diagnostics Nederland BV, Almere, the Netherlands) at −80˚C. Solutions were overnight spun at 4˚C and thereafter centrifuged at 1,700 rpm for 15 minutes. Pellet and supernatant were collected separately for each tissue (NP and AF) and stored until use at −20˚C. Pellets were digested overnight at 60˚C in papain buffer (250 μg/mL papain, P3125-100 mg, Sigma-Aldrich with 1.57 mg/mL cysteine HCL, C7880, Sigma-Aldrich). GAG content was quantified by the 1,9-dimethylmethylene blue (DMMB) assay [44]. Chondroitin sulfate from shark cartilage (C4384, Sigma-Aldrich) was used as a standard to calculate GAG concentrations and the ratio of absorption at 540 to 595 nm was measured by a microplate reader (Multimode detector DTX 880, Beckman Coulter). DNA content was determined using a Quant-iT dsDNA Broad-Range assay kit in combination with Qubit fluorometer (Invitrogen, Paisley, UK) in accordance with the manufacturer's instructions.

Hydroxyproline content was determined using a colometric assay. Hundred microliter papain-digested tissue pellets were dried by the evaporation of the solvent in a cooled speed vac and subsequently hydrolyzed in 100 μL 4 M NaOH for 24 hours at 108˚C. Hydrolysis was stopped by adding 100 μL 1.4 M citric acid, vortexed, and centrifuged for 15 seconds at 14,000 rpm. Then, 35 μL supernatant was dispensed into a 96-well plate, followed by 75 μL assay buffer with chloramine T reagent (2426, Merck, Schiphol-Rijk, the Netherlands) and incubated for 20 minutes on a shaker at 170 rpm. Seventy-five microliter dimethylaminobenzaldehyde (3058 Merck) was freshly added and incubated for 20 minutes at 60˚C and cooled down before the absorbance was read at 570 nm. Collagen content was calculated from the hydroxyproline content by multiplying by 7.5 [45]. GAG and collagen content were normalized to DNA content for both NP and AF tissues. Also, GAG was normalized to collagen to evaluate the ratio between these tissues.

ELISA for PGE_2 and TAA tissue content. The supernatants of the above-mentioned tissue digests were used for analysis of TAA (as a measure of presence of TAA released by the PEAMs at 12 weeks follow-up) and PGE_2 content (as a measure of TAA bioactivity upon release from the PEAMs) using a competitive colometric ELISA

Table 3
Details of the immunohistochemistry protocols used

First antibody	Work concentration	Origin	Antigen retrieval	Block	Washing	Second antibody
Collagen type I (ab6308, Abcam, Cambridge, UK)	0.1 μg/mL	Mouse monoclonal	1 mg/mL pronase for 30 min at 37˚C 10 mg/mL HA for 30 min at 37˚C	S2003, Dako, USA PBS+5% BSA	PBS+0.1% Tween20	EnVision+System-HRP Goat Anti-Mouse, K4001, Dako, Glostrup, Denmark
Collagen type II (II-II6B3, DSHB, Iowa City, IA)	0.4 μg/mL	Mouse monoclonal	1 mg/mL pronase for 30 min at 37˚C 10 mg/mL HA for 30 min at 37˚C	S2003, Dako, USA PBS+5% BSA	PBS+0.1% Tween20	EnVision+System-HRP Goat Anti-Mouse, K4001, Dako, Glostrup, Denmark
Collagen type X (art 1-CO097-05, Quartett, Germany)	50 μg/mL	Mouse monoclonal	0.1% pepsin for 20 min at 37˚C 10 mg/mL HA for 30 min at 37˚C	S2003, Dako, USA PBS+10% normal goat serum	PBS+0.1% Tween20	EnVision+System-HRP Goat Anti-Mouse, K4001, Dako, Glostrup, Denmark
Normal mouse IgG1 (3877, Santa Cruz Biotechnology, Heidelberg, Germany)	*	Mouse	*	*	*	*
NGF (ab6198, Abcam, Cambridge, UK)	1.25 μg/mL	Rabbit polyclonal antibody	10 mM Na citrate pH 6.0 water bath for 20 min at 80˚C		TBS+0.1% Tween20	EnVision+System-HRP Goat Anti-Rabbit, K4011, Dako, Glostrup, Denmark
Normal rabbit IgG1 (1.25 μg/mL; X0903, Dako, Glostrup, Denmark	*	Rabbit	*		*	*

BSA, bovine serum albumin; HA, hyaluronidase; HRP, horseradish peroxidase; IgG, Immunoglobulin G; NGF, nerve growth factor; PBS, phosphate buffered saline; TBS, tris buffered saline.
* same as first antibody of interest.

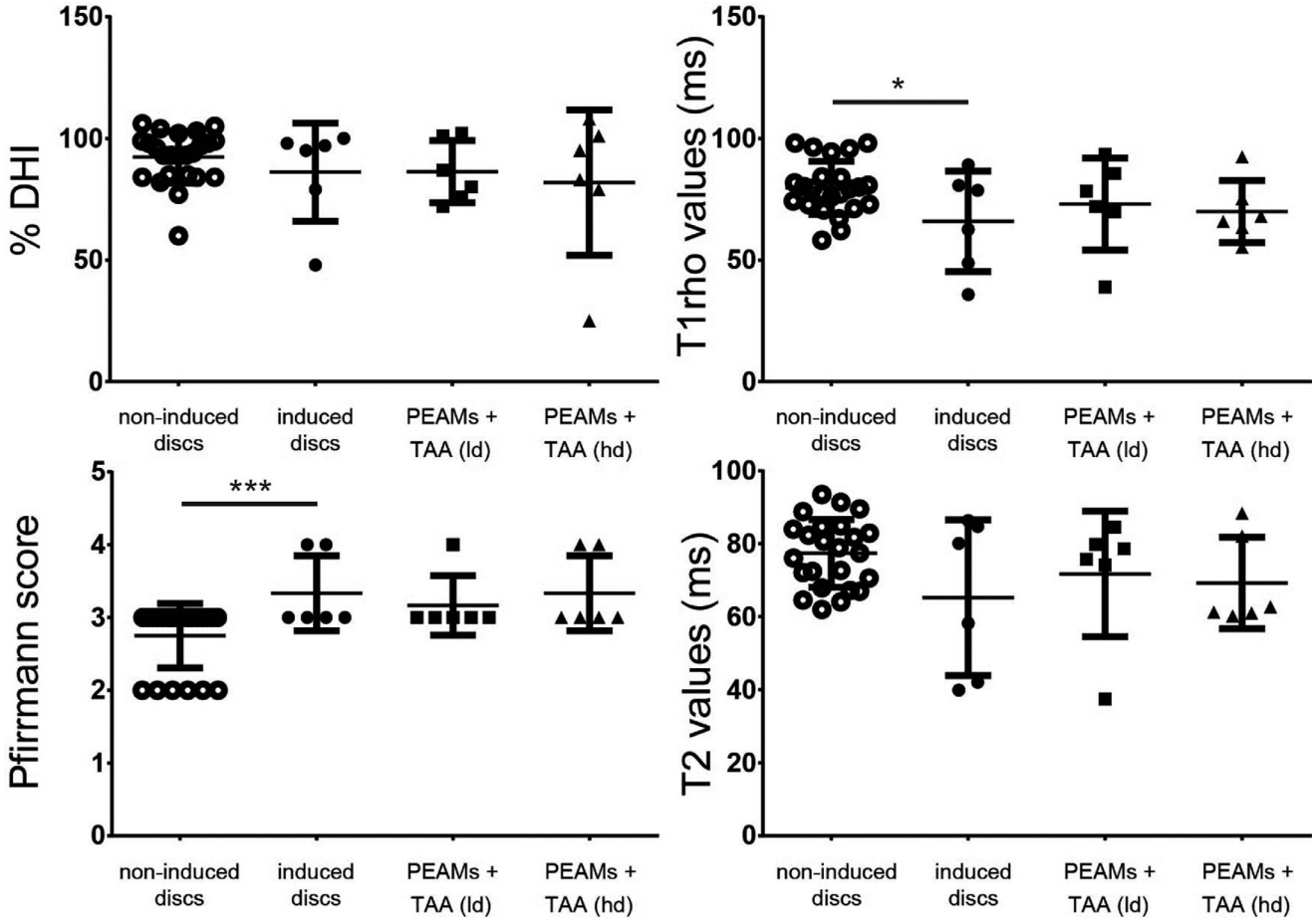

Fig. 1. Disc height index (DHI), Pfirrmann grades and nucleus pulposus (NP) T1ρ, T2-weighted values of IVDs where further degeneration was induced and treated with TAA, compared with noninduced controls. Noninduced discs, healthy control; induced discs, nucleotomy-induced degenerated discs; PEAMs, poly(esteramide) microspheres; TAA, triamcinolone acetonide; ld, low dosage (8.4 μg); hd, high dosage (0.84 mg). *p<0.05 and ***p<0.001.

(Prostaglandin E_2 monoclonal ELISA kit, Cayman Chemical, Ann Arbor, MI and TAA ELISA #105119, Neogen, UK) in accordance with the manufacturer's instructions. PGE_2 content was normalized for DNA content of NP and AF tissues.

Statistical analysis. All data were analyzed using IBM SPSS Statistics software (version 21). All mean outcome values of non-nucleotomized discs were compared with nucleotomy-induced degenerated discs at time points t_0 and t_{12} with independent sample *t* tests. In the treatment groups (induced, TAA ld and TAA hd) equality of data variances was evaluated by Q–Q plots and homoscedasticity of residuals by scatterplots. In case these assumptions were not met, data were logarithmically transformed, otherwise the Kruskal-Wallis test was used to analyze nonparametric data (TAA retention, T1ρ values, and Thompson score). For each tissue (NP and AF separately), GAG values were normalized for DNA and collagen for GAG content for all groups, and means were compared with each other using a randomized block design ANOVA to correct for donor variability. If statistical significant differences were found between groups, Tukey's post hoc analysis was used to correct for multiple comparisons. NGF immunopositive cell averages were analyzed with independent sample *t* test, Bonferroni post hoc analysis was used to correct for multiple comparisons (induced vs. TAA ld and induced vs. TAA hd). Statistical significance was assumed for $p<0.05$.

Results

All dogs recovered from surgery uneventfully and remained without evident clinical disorders during the 12-week study period.

Triamcinolone acetonide administration did not alter intervertebral disc degeneration progression

In nucleotomy-induced degenerated IVDs, progressive degeneration was seen as confirmed by Pfirrmann scores (Fig. 1, $p<0.001$) and reduction of the T1ρ values. Disc height remained unaltered at 12 weeks follow-up regardless of the treatment group (Fig. 1) consistent with mild degeneration. Quantitative T1ρ and T2 values

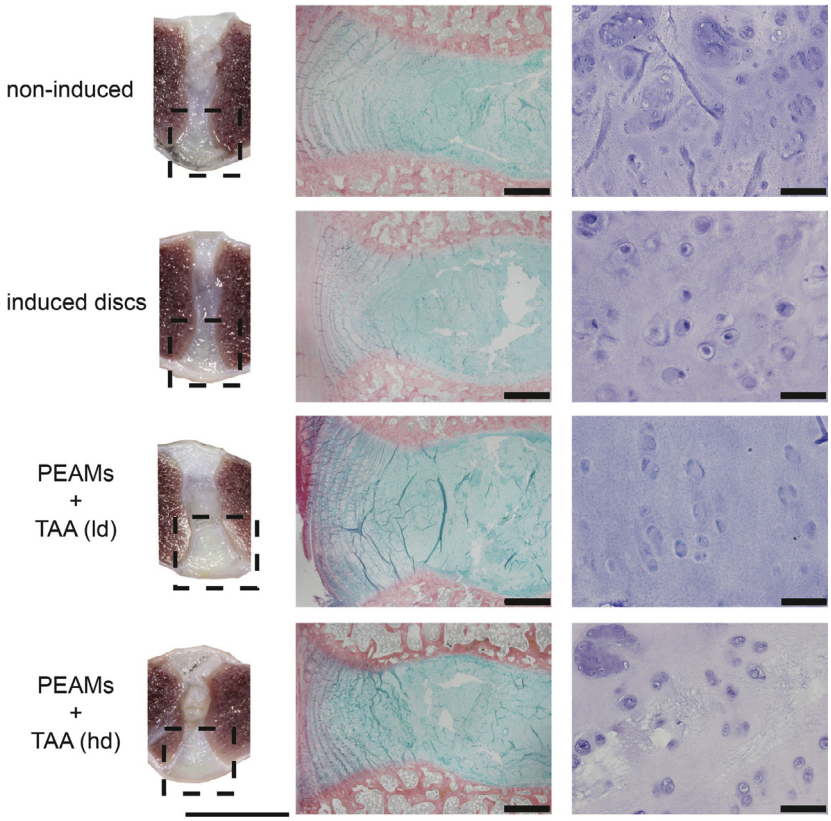

Fig. 2. Representative macroscopic mid-sagittal images of intervertebral discs (left column), squared boxes indicate location of region depicted for histology. Scale bar = 1 cm. Microscopic images of ventral annulus fibrosus and nucleus pulposus stained with picosirius red/alcian blue to visualize collagens and proteoglycans, respectively (middle column). Scale bar = 1 mm. Microscopic images of nucleus pulposus stained with hematoxylin and eosin (right column). Scale bar = 50 μm. Noninduced discs, healthy control; induced discs, nucleotomy-induced degenerated discs; PEAMs, poly(esteramide) microspheres; TAA, triamcinolone acetonide; ld, low dosage (8.4 μg); hd, high dosage (0.84 mg).

showed no difference in IVD degeneration between treatments at the end point of the study (Fig. 1). No abnormalities that were treatment related were observed on CT images postmortem. Some sclerosis of the endplates and very mild new bone formation occurred occasionally (2/6 levels) at the location of degeneration induction, independent of the treatment, probably due to minor surgical trauma (data not shown). Macroscopic and microscopic analyses showed no evidence of osteoporosis. Furthermore, macroscopic and microscopic evaluation and scoring at 12 weeks follow-up showed no clear differences in degeneration or tissue integrity 12 weeks after TAA administration (Figs. 2 and 3).

Triamcinolone acetonide detection in intervertebral disc tissue 12 weeks after intradiscal injection

Approximately one-fourth of the NP and AF tissue of each IVD was employed to determine TAA levels from tissue extracts. NP tissue from IVDs injected with empty microspheres did not contain appreciable levels of TAA (data not shown). TAA was detected in AF tissue of IVDs injected with TAA containing microspheres, 12 weeks after injection (Fig. 4, $p<0.05$). No difference was noted between the two dosages.

Extracellular matrix (immuno)histology

Histologic evaluation of the NP and AF revealed that collagen type I was absent in the ECM of NP and inner AF tissues for all conditions as depicted in Fig. 5 compatible with mild degeneration. In nucleotomy-induced degenerated IVDs injected with empty PEAMs, collagen type II was present only pericellularly in the NP, compared with IVDs injected with TAA low dosage and TAA high dosage, where collagen type II was also found in the ECM. Collagen II was observed throughout the AF in all conditions (Fig. 5). Collagen type X was absent in the ECM of all IVDs (data not shown), while the canine growth plate (positive control) stained appropriately.

Local delivery of triamcinolone acetonide-loaded microspheres did not affect extracellular matrix content

Degeneration in nucleotomy-induced degenerated IVDs as measured by Pfirrmann scoring was not reflected by

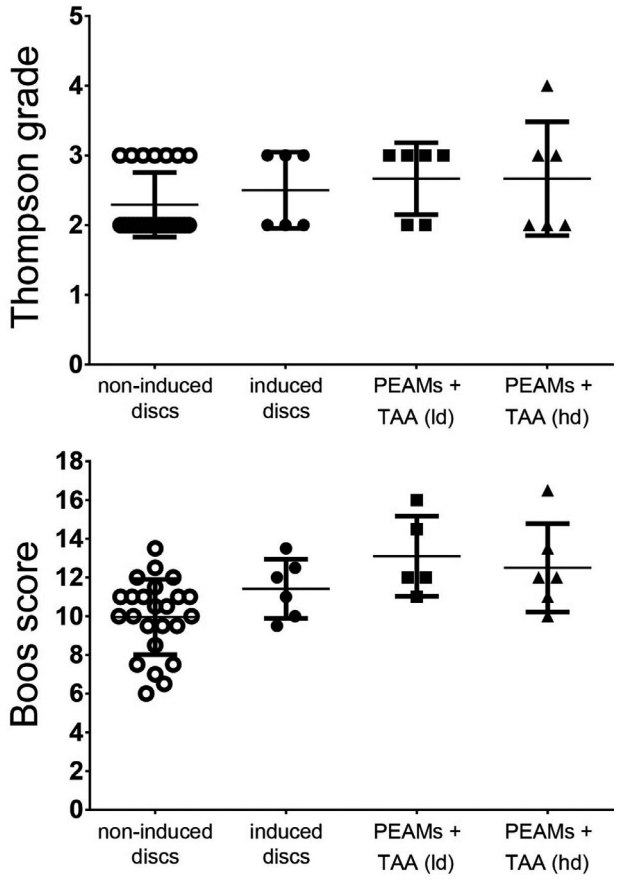

Fig. 3. Macroscopic (Thompson) grade and microscopic (Boos) scoring systems were applied to evaluate IVD degeneration. Noninduced discs, healthy control; induced discs, nucleotomy-induced degenerated discs; PEAMs, poly(esteramide) microspheres; TAA, triamcinolone acetonide; ld, low dosage (8.4 μg); hd, high dosage (0.84 mg).

GAG/DNA or GAG/collagen content of the NP. Levels did not differ from non-nucleotomized levels at 12 weeks follow-up (Fig. 6), nor were these affected by TAA delivery. TAA exposure did not significantly influence PGE_2/DNA levels in NP tissue (Fig. 6). In contrast to NP tissue, GAG/DNA levels were decreased and PGE_2/DNA levels increased in AF tissues 4 weeks after induction of degeneration (Fig. 6, $p<0.05$). GAG/collagen ratio however was not affected in nucleotomy-induced degenerated AF tissue. Extended TAA release did not result in significant differences in GAG/collagen ratios compared with induced or non-induced IVDs in AF tissues (Fig. 6). TAA exposure did not alter PGE_2/DNA levels in AF tissue (Fig. 6).

Nerve growth factor was decreased in nucleus pulposus tissues treated with triamcinolone acetonide

Increased NGF levels are associated with inflammation and chronic LBP [9], and NGF released by degenerated NP cells can contribute to the innervation of the degenerated IVD [46]. Therefore, the presence of NGF

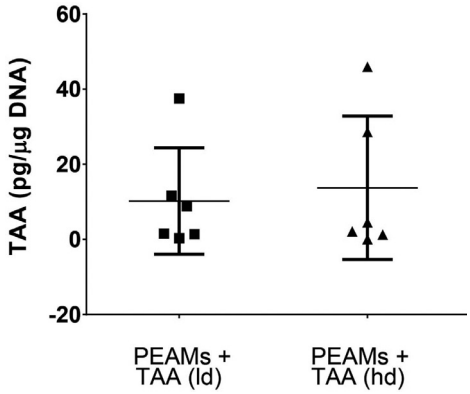

Fig. 4. TAA retention in annulus fibrosus after 12 weeks of intradiscal delivery. TAA was measured in induced discs injected with PEAMs+TAA low dosage (ld) and PEAMs+TAA high dosage (hd). Amount of TAA was corrected for DNA content of each annulus fibrosus. TAA was still detected in most of the induced discs injected with PEAMs+TAA. PEAMs, poly(esteramide) microspheres; TAA, triamcinolone acetonide.

in NPs of nucleotomy-induced degenerated IVDs after exposure to extended TAA release was further investigated (Fig. 7). On average, nucleotomy-induced degenerated IVDs (56±6.8%) contained significantly more NGF immunopositive NP cells compared with non-nucleotomized controls (15±3.9%; Fig. 7, $p<0.001$). In the NP of IVDs exposed to the lower dosage of TAA, significantly less NGF immunopositive cells were present (30±4.0%) compared with nucleotomy-induced degenerated IVDs (Fig. 7, $p<0.05$). Although not statistically significant, also in nucleotomy-induced degenerated IVDs treated with the higher dosage of TAA, less cells (42±5.6%) were immunopositive for NGF compared with non-nucleotomized controls (15±3.9%).

Discussion

This is the first study to show the safety of intradiscal delivery and extended release of TAA in a clinically relevant large animal model recapitulating the process of disc degeneration in man [47]. TAA was still detectable 12 weeks after intradiscal delivery confirming local, sustained and prolonged drug delivery by the PEAMs and did not affect IVD or bone integrity, based on macroscopic evaluation, disc height index, T1ρ and T2 values, and histopathologic and biochemical analyses. Prolonged TAA exposure at the lower dosage decreased NGF immunopositivity in NP tissue from nucleotomy-induced degenerated IVDs, indicative of an analgesic effect, although the setup of the current study did not allow for pain as a readout parameter.

Needle puncture of the IVD is required for local delivery of therapeutic agents, but has been suggested to induce IVD degeneration [48–50]. This was mainly based on one publication where discography was shown to enhance degeneration in human subjects. However, this seemed to have mainly occurred in healthy IVDs [50]. Moreover, discography involves pressurization of the IVD and the contrast

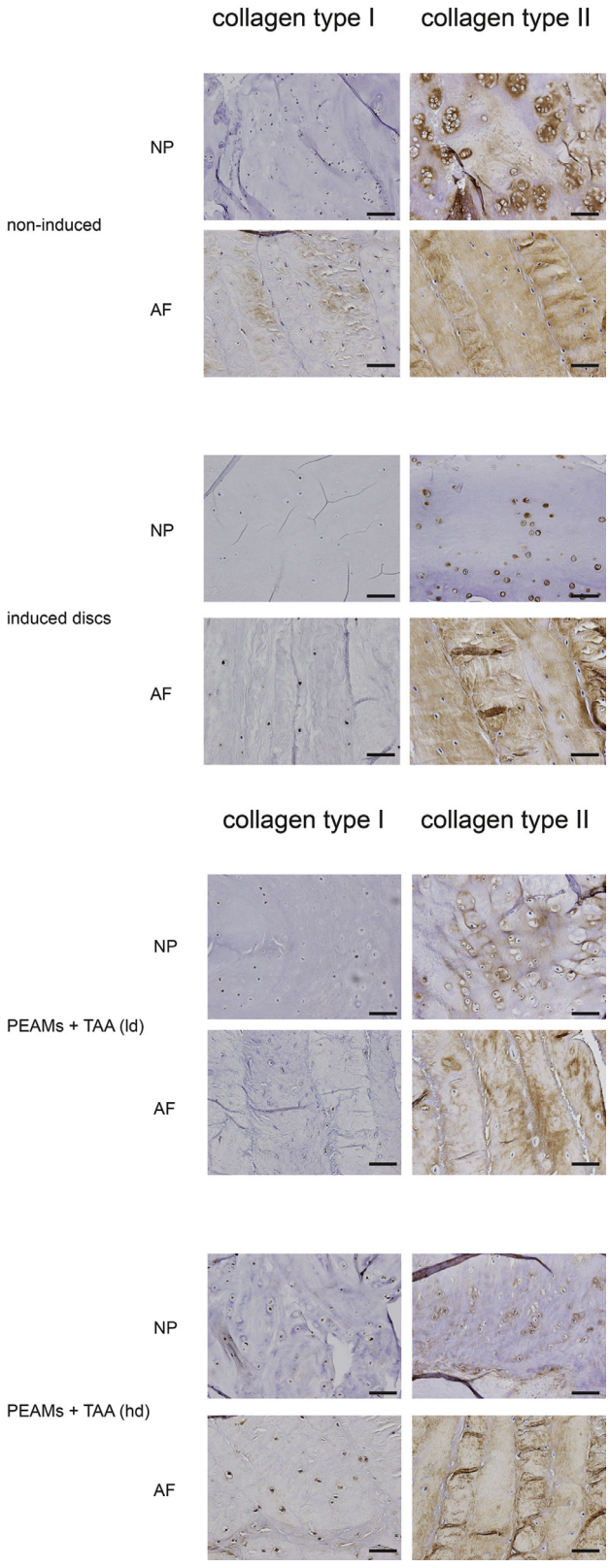

Fig. 5. Immunohistologic staining for collagen types I and II of nucleus pulposus (NP) and annulus fibrosus (AF) tissues. Collagen type I, scale bar = 50 μm and collagen type II, scale bar = 20 μm. Non-induced discs, healthy control; induced discs, nucleotomy-induced degenerated discs; PEAMs, poly(esteramide) microspheres; TAA, triamcinolone acetonide; ld, low dosage (8.4 μg); hd, high dosage (0.84 mg).

agent used has been shown to reduce IVD cell proliferation and enhance cell death [51,52]. As previous large animal studies in which small volumes of noncytotoxic materials were injected in mildly degenerated IVDs showed no long-term damage to the injected IVD [32–34], the two former factors rather than insertion of a needle itself will have entailed the described risk. Although needle puncture is applied to induce IVD degeneration in small experimental animal models [49,53], this is dependent on the needle size relative to the IVD size [49]. In large animal studies [32–34,47], the use of 27G needles was shown safe, but in rat IVDs, insertion of a 27G needle induced degeneration [49]; this would be comparable to injection of a human IVD with a needle larger than 6G (6.4 mm). Nevertheless, the exact cutoff for needle size for safe injection in the human IVD still warrants further investigation. It is therefore unlikely that the degenerative changes observed in this study are attributed to needle puncture of the IVD.

Intradiscal glucocorticoid injections in human patients have been investigated extensively before with pain relief as major aim and outcome parameter [18–21,54,55]. However, the toxic formulations of steroid depots containing PEG, carboxymethylcellulose or benzyl alcohol, might have been an underappreciated confounder in these studies [25,56]. Considering that TAA depot formulations also consist of the latter, negative results from previous clinical studies using these formulations may be attributed to the excipients rather than the corticosteroids [26,57]. In the current study, nontoxic PEAMs [34,58] were used to deliver a relatively high dosage of TAA in the IVD without additional excipients. Considering that the high dosage of TAA (0.84 mg) delivered to the canine IVD is the maximum attainable dosage and slightly under the human dosage used for other corticosteroid preparations for intradiscal injections, this platform appears to provide the opportunity to deliver local high dosages of TAA without adding toxic compounds to the formulation. Also, TAA crystallization, which can also be toxic when in direct contact with cells [57,59], is less likely to occur when using a slowly degrading biomaterial depot like PEAMs. Both the PEA biomaterial platform and controlled release of glucocorticoids have been shown to be safe in other tissues [34–36]. Other side effects of long-term glucocorticoid delivery may be osteoporosis [60]. In this study, the TAA released by the PEAM platform did not influence bony structures, as was determined by CT evaluation and histologic examination of the cortical and trabecular bones. Considering that TAA was still detectable in the IVD 12 weeks after administration, apparently relatively high dosages of TAA can be locally delivered using controlled release formulations without exerting detrimental effects. Interestingly, TAA was not detected in NP tissues from nucleotomy-induced degenerated IVDs injected with TAA releasing microspheres. This may be due to the limited amount of tissue available for extraction and analysis (1/4 IVD) combined with TAA levels in the NP around the detection limit. On the other hand,

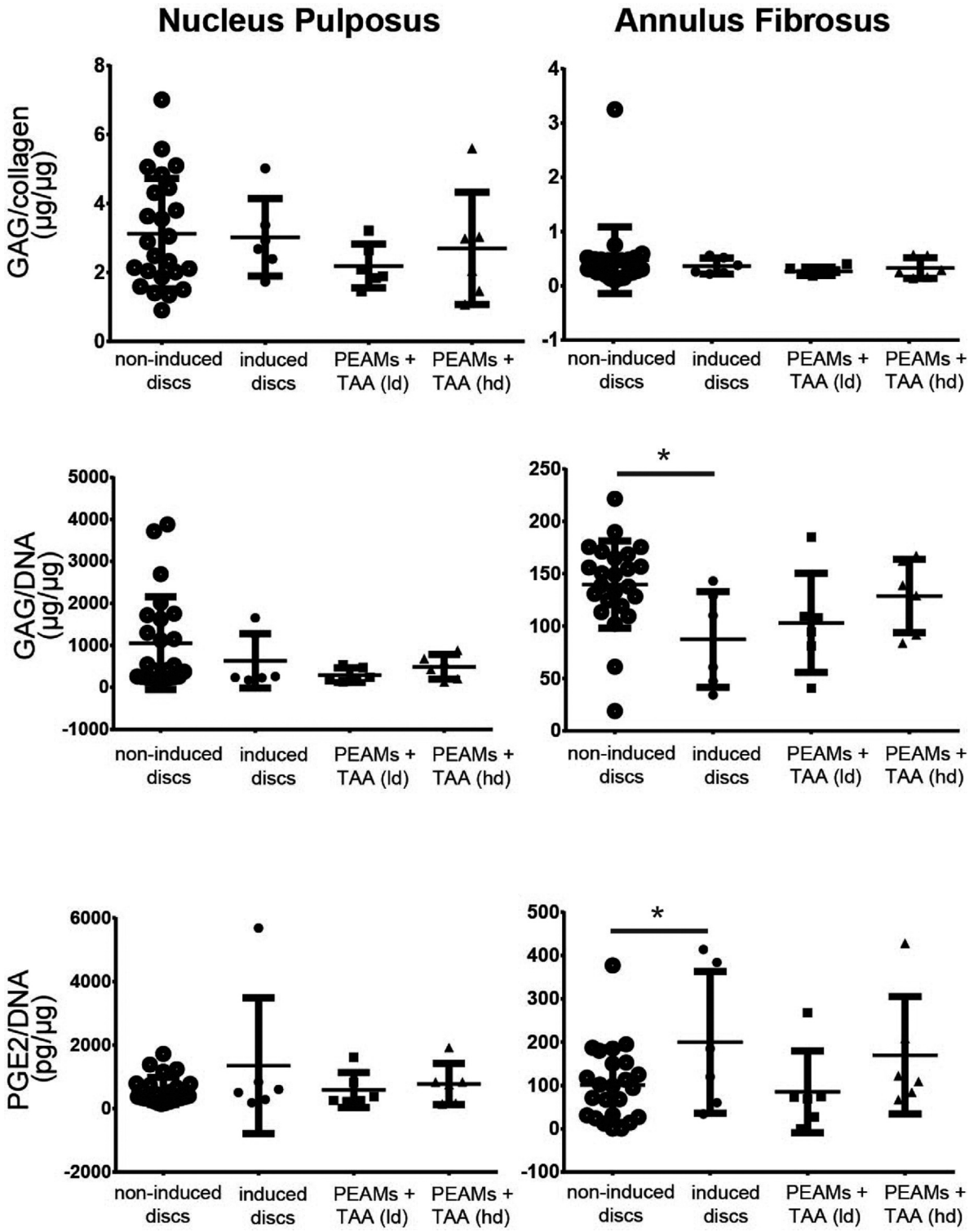

Fig. 6. Glycosaminoglycan (GAG) corrected for collagen or DNA content and prostaglandin E2 (PGE_2) corrected for DNA, in both nucleus pulposus and annulus fibrosus tissues. Noninduced discs, healthy control; induced discs, nucleotomy-induced degenerated discs; PEAMs, poly(esteramide) microspheres; TAA, triamcinolone acetonide; ld, low dosage (8.4 μg); hd, high dosage (0.84 mg). *p<0.05.

TAA is known to bind to proteins [61], thereby extending its half-life and therapeutic duration, as has been shown for ocular pigments in applications for eye diseases [62]. Hence, another possible explanation for the presence of TAA in the AF opposed to the NP might be the binding of TAA to ECM proteins, which are more abundantly present in the AF than in the NP. However, this binding has never been subject of investigation.

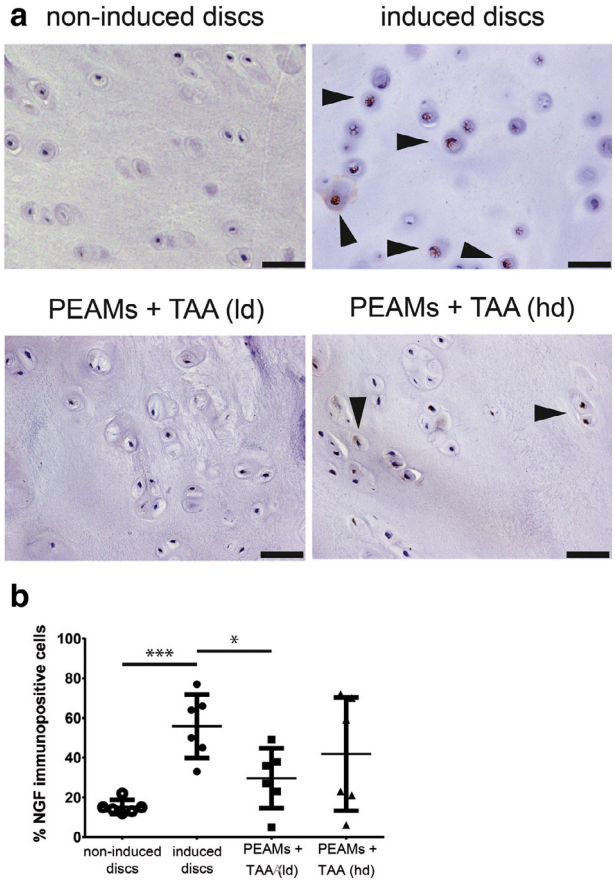

Fig. 7. Immunohistologic staining for nerve growth factor (NGF). (a) Histologic image of nucleus pulposus (NP) cells, NGF immunopositivity is indicated by the black arrows. Scale bar = 50 μm. (b) Quantification of NGF immunopositive NP cells. Noninduced discs, healthy control; induced discs, nucleotomy-induced degenerated discs; PEAMs, poly(ester-amide) microspheres; TAA, triamcinolone acetonide; ld, low dosage (8.4 μg); hd, high dosage (0.84 mg). *p<0.05 and ***p<0.001.

To our knowledge, the effect of sustained local TAA release on IVD tissue in a clinically relevant larger animal model has not been investigated before. So far, only one study described the effect of the controlled release of corticosteroids, that is, cortisone, from ceramic capsules in a rat IVD degeneration model. The implanted ceramic capsules releasing the corticosteroid delayed progression of stab-induced degeneration after 4 weeks compared with empty capsules, as was determined by increased disc height and increased cell density [28]. However, the latter is also a hallmark for degeneration in humans and canines [42,63]. Moreover, rat tail IVDs are not well comparable to lumbar IVDs, due to differences in size, cell composition, and mechanical loading [64]. At the cellular level, corticosteroid exposure has shown to have mixed effects. Human IVD cell proliferation in pellet culture was suppressed in the presence of TAA, although GAG and collagen content was not affected [65]. Dexamethasone stimulated bovine NP and AF cell proliferation in monolayer culture [66], in contrast to its effects found in 3D culture systems used in other studies [67,68]. In the current study, even the relatively high dosage of TAA did not induce further degeneration of nucleotomy-induced IVDs, as was assessed by MRI, macroscopic, microscopic, and biochemical evaluation. Even so, prolonged TAA exposure could not slow down progression of degeneration 12 weeks after intradiscal delivery based on all the outcomes. However, in the present study, the degeneration induced by nucleotomy was mild (Pfirrmann grade III; supplementary Fig. 1). Furthermore, non-nucleotomized and nucleotomy-induced degenerated IVDs also did not differ significantly at the biochemical and histologic ECM content and tissue PGE_2 levels, even 16 weeks after induction of degeneration, except for decreased GAG/DNA levels in the AF of induced IVDs. As such, our study may be underpowered to detect significant biochemical and structural effects of TAA exposure in the degenerating IVD. Possibly after nucleotomy, intrinsic disc repair occurs and biochemical levels normalize over a longer period of time [53].

From a clinical perspective, the present platform seems to be promising in extending the local controlled delivery of TAA with the potency to provide long-standing analgesia in the subset of LBP patients suffering from discogenic pain. Clinical efficacy in pain reduction could not be determined, given that the present model employed a randomized block design to comply with the 3Rs principles and degeneration remained at the subclinical level. However, at the IVD tissue level, we did observe inhibition of NGF protein expression, which was statistically significant for the lower dosage of TAA. Although the lack of significance found for the NGF decrease in the high dosage-treated IVDs implies a dose dependency, rather the limited number of IVDs in each group and the inherently large biological variation found in this type of model may have been the culprit. NGF protein expression is thought to play a role in the development of painful IVDs by the stimulation of peripheral nociceptive sensory neuron growth into degenerated IVDs [9,69] and pain sensitization [10,11]. It has been suggested that local chemical factors, such as PGE_2, in the IVD and nerves might render IVDs painful via spontaneous firing of the nerve roots [70,71]. Nerve roots were shown to increase their firing pattern upon PGE_2 stimulation, which can in turn be inhibited by TAA [72]. However, no effect of TAA was found on PGE_2 levels, possibly due to the minimally elevated PGE_2 levels in nucleotomy-induced degenerated NP tissues, which was only statistically significant in the AF. Therefore, further suppression of PGE_2 by TAA may have been impossible. NGF expression in the NP, however, did decrease after prolonged TAA exposure in nucleotomy-induced degenerated IVDs, by as yet unidentified mechanisms of action. One possible explanation for the discrepancy between inflammatory and pain marker expression NP levels is that the inflammation upon induction may have been increased temporarily, whereas the resulting pain response in the IVD may have been chronic. The interaction between PGE_2 and NGF is not completely understood and

sometimes their production indeed diverges. Patients experiencing pain in different body structures do not always show increased inflammation, as detected by PGE_2 production [73–75]. NGF production has been shown to much more closely correlate with pain than inflammation in several patient populations [73,75]. In line with this, anti-NGF treatments have shown promise in pain relief in chronic LBP patients [76] and as TAA can reduce NGF expression in degenerated IVDs, this may be a cost-effective alternative to such expensive biologicals-based treatments. As IVD degeneration processes and chronic LBP are common and comparable in dogs and humans, the current preclinical large animal model may also be used as proof of principle in the treatment of canine patients with LBP [31]. Therefore, to confirm clinical efficacy on pain reduction of the controlled release of TAA by the PEA platform, a study design in clinical trial setting with client-owned dogs or human patients would be a logical next step, taking this product a step closer to the bedside of human patients. As no clear effects were noted on IVD degeneration, the release of coadministered regenerative factors is a route worthwhile investigating in the near future [29,77].

In conclusion, controlled release of TAA did not affect degeneration in the nucleotomy-induced degenerated IVDs, nor were side effects found. As NGF production was decreased, extended TAA release holds promise in treating pain associated with IVD degeneration.

Acknowledgments

This research was funded by a research grant from Health Holland/Life Sciences & Health (ArIADNE; project no 40-43100-98-022). Also the financial contribution of the Dutch Arthritis Foundation is gratefully acknowledged (LLP12 and LLP22). Furthermore, we like to thank Saskia Plomp for technical assistance.

Supplementary materials

Supplementary material associated with this article can be found, in the online version, at doi:10.1016/j.spinee.2018.10.014.

References

[1] Luoma K, Riihimaki H, Luukkonen R, Raininko R, Viikari-Juntura E, Lamminen A. Low back pain in relation to lumbar disc degeneration. Spine 2000;25:487–92.

[2] Murray CJ, Vos T, Lozano R , Naghavi M, Flaxman AD, Michaud C. et al. Disability-adjusted life years (DALYs) for 291 diseases and injuries in 21 regions, 1990-2010: a systematic analysis for the Global Burden of Disease Study 2010. Lancet 2012;380:2197–223.

[3] Sheng B, Feng C, Zhang D, Spitler H, Shi L. Associations between obesity and spinal diseases: a medical expenditure panel study analysis. Int J Environ Res Public Health 2017;14:183–94.

[4] Antoniou J, Steffen T, Nelson F, et al. The human lumbar intervertebral disc: evidence for changes in the biosynthesis and denaturation of the extracellular matrix with growth, maturation, ageing, and degeneration. J Clin Invest 1996;98:996–1003.

[5] Liebscher T, Haefeli M, Wuertz K, Nerlich AG, Boos N. Age-related variation in cell density of human lumbar intervertebral disc. Spine 2011;36:153–9.

[6] Roughley PJ. Biology of intervertebral disc aging and degeneration: involvement of the extracellular matrix. Spine (Phila Pa 1976) 2004;29:2691–9.

[7] Morgan FP, King T. Primary instability of lumbar vertebrae as a common cause of low back pain. J Bone Joint Surg Br 1957;39-B:6–22.

[8] Allegri M, Montella S, Salici F, Valente A, Marchesini M, Compagnone C. et al. Mechanisms of low back pain: a guide for diagnosis and therapy. F1000Res 2016;5.

[9] Freemont AJ, Peacock TE, Goupille P, Hoyland JA, O'Brien J, Jayson MI. Nerve ingrowth into diseased intervertebral disc in chronic back pain. Lancet 1997;350:178–81.

[10] Binch AL, Cole AA, Breakwell LM, Michael AL, Chiverton N, Cross AK. et al. Expression and regulation of neurotrophic and angiogenic factors during human intervertebral disc degeneration. Arthritis Res Ther 2014;16:416.

[11] Krock E, Rosenzweig DH, Chabot-Dore AJ, Jarzem P, Weber MH, Ouellet JA. et al. Painful, degenerating intervertebral discs up-regulate neurite sprouting and CGRP through nociceptive factors. J Cell Mol Med 2014;18:1213–25.

[12] Chou R, Huffman LH. American Pain Society, American College of Physicians. Medications for acute and chronic low back pain: a review of the evidence for an American Pain Society/American College of Physicians clinical practice guideline. Ann Intern Med 2007;147:505–14.

[13] Chung JW, Zeng Y, Wong TK. Drug therapy for the treatment of chronic nonspecific low back pain: systematic review and meta-analysis. Pain Physician 2013;16:E685–704.

[14] Rehman Q, Lang T, Modin G, Lane NE. Quantitative computed tomography of the lumbar spine, not dual x-ray absorptiometry, is an independent predictor of prevalent vertebral fractures in postmenopausal women with osteopenia receiving long-term glucocorticoid and hormone-replacement therapy. Arthritis Rheum 2002;46:1292–7.

[15] Lian KC, Lang TF, Keyak JH, Modin GW, Rehman Q, Do L. et al. Differences in hip quantitative computed tomography (QCT) measurements of bone mineral density and bone strength between glucocorticoid-treated and glucocorticoid-naive postmenopausal women. Osteoporos Int 2005;16:642–50.

[16] Lukert BP, Raisz LG. Glucocorticoid-induced osteoporosis: pathogenesis and management. Ann Intern Med 1990;112:352–64.

[17] Cao P, Jiang L, Zhuang C , Yang Y, Zhang Z, Chen W. et al. Intradiscal injection therapy for degenerative chronic discogenic low back pain with end plate Modic changes. Spine J 2011;11:100–6.

[18] Khot A, Bowditch M, Powell J, Sharp D. The use of intradiscal steroid therapy for lumbar spinal discogenic pain: a randomized controlled trial. Spine (Phila Pa 1976) 2004;29:833–6. discussion 837.

[19] Simmons JW, McMillin JN, Emery SF, Kimmich SJ. Intradiscal steroids. A prospective double-blind clinical trial. Spine (Phila Pa 1976) 1992;17(Suppl. 6):S172–5.

[20] Ito S, Usui H, Maruyama K, Muro T. Roentgenographic evaluation of ossification and calcification of the lumbar spinal canal after intradiscal betamethasone injection. J Spinal Disord 2001;14:434–8.

[21] Nguyen C, Benichou M, Revel M, Poiraudeau S, Rannou F. Association of accelerated switch from vertebral end-plate Modic I to Modic 0 signal changes with clinical benefit of intradiscal corticosteroid injection for chronic low back pain. Arthritis Rheum 2011;63:2828–31.

[22] Buttermann GR. The effect of spinal steroid injections for degenerative disc disease. Spine J 2004;4:495–505.

[23] Gullbrand SE, Peterson J, Mastropolo R, Roberts TT, Lawrence JP, Glennon JC. et al. Low rate loading-induced convection enhances net transport into the intervertebral disc in vivo. Spine J 2015;15:1028–33.

[24] Aoki M, Kato F, Mimatsu K, Iwata H. Histologic changes in the intervertebral disc after intradiscal injections of methylprednisolone acetate in rabbits. Spine (Phila Pa 1976) 1997;22:127–31. discussion 132.
[25] Candido KD, Knezevic I, Mukalel J, Knezevic NN. Enhancing the relative safety of intentional or unintentional intrathecal methylprednisolone administration by removing polyethylene glycol. Anesth Analg 2011;113:1487–9.
[26] Zhengyu S, Fang W, Ying F. Vehicle used for triamcinolone acetonide is toxic to ocular tissues of the pigmented rabbit. Curr Eye Res 2009;34:769–76.
[27] Menkes CJ, Vallee C, Giraudet-Le Quintrec JS. Calcification of the epidural space following an intradiscal injection of triamcinolone hexacetonide. Presse Med 1989;18:1707.
[28] Ragab AA, Woodall JW, Tucci M.A. Jr, Wingerter SA, Fosnaugh AW, Franklin LN. et al. A preliminary report on the effects of sustained administration of corticosteroid on traumatized disc using the adult male rat model. J Spinal Disord Tech 2009;22:473–8.
[29] Liang CZ, Li H, Tao YQ, Peng LH, Gao JQ, Wu JJ. et al. Dual release of dexamethasone and TGF-beta3 from polymeric microspheres for stem cell matrix accumulation in a rat disc degeneration model. Acta Biomater 2013;9:9423–33.
[30] Nair AB, Jacob S. A simple practice guide for dose conversion between animals and human. J Basic Clin Pharm 2016;7:27–31.
[31] Bergknut N, Rutges JP, Kranenburg HJ, Smolders LA, Hagman R, Smidt HJ. et al. The dog as an animal model for intervertebral disc degeneration? Spine (Phila Pa 1976) 2012;37:351–8.
[32] Tellegen AR, Willems N, Beukers M, et al. Intradiscal application of a PCLA-PEG-PCLA hydrogel loaded with celecoxib for the treatment of back pain in canines: what's in it for humans? J Tissue Eng Regen Med 2018;12:642–52.
[33] Willems N, Yang HY, Langelaan ML, et al. Biocompatibility and intradiscal application of a thermoreversible celecoxib-loaded poly-N-isopropylacrylamide MgFe-layered double hydroxide hydrogel in a canine model. Arthritis Res Ther 2015;17:214.
[34] Willems N, Mihov G, Grinwis GC, et al. Safety of intradiscal injection and biocompatibility of polyester amide microspheres in a canine model predisposed to intervertebral disc degeneration. J Biomed Mater Res B Appl Biomater 2015;105B:707–14.
[35] Andres-Guerrero V, Zong M, Ramsay E, et al. Novel biodegradable polyesteramide microspheres for controlled drug delivery in Ophthalmology. J Control Release 2015;211:105–17.
[36] Rudnik-Jansen L, Colen S, Berard J, Plomp S, Que I, van Rijen M. et al. Prolonged inhibition of inflammation in osteoarthritis by triamcinolone acetonide released from a polyester amide microsphere platform. J Control Release 2017;253:64–72.
[37] Katsarava R, Beridze V, Arabuli N, Kharadze D, Chu C, Won C. Amino acid-based bioanalogous polymers. Synthesis, and study of regular poly(ester amide)s based on bis(a-amino acid) a,v-alkylene diesters, and aliphatic dicarboxylic acids. J Polym Sci: Part A: Polym Chem 1999;37:391–407.
[38] Bergknut N, Smolders LA, Grinwis GC, Hagman R, Lagerstedt AS, Hazewinkeld HA. et al. Intervertebral disc degeneration in the dog. Part 1: anatomy and physiology of the intervertebral disc and characteristics of intervertebral disc degeneration. Vet J 2013;195:282–91.
[39] Bergknut N, Auriemma E, Wijsman S, Voorhout G, Hagman R, Lagerstedt AS. et al. Evaluation of intervertebral disk degeneration in chondrodystrophic and nonchondrodystrophic dogs by use of Pfirrmann grading of images obtained with low-field magnetic resonance imaging. Am J Vet Res 2011;72:893–8.
[40] Willems N, Bach FC, Plomp SG, van Rijen MH, Wolfswinkel J, Grinwis GC. et al. Intradiscal application of rhBMP-7 does not induce regeneration in a canine model of spontaneous intervertebral disc degeneration. Arthritis Res Ther 2015;17:137.
[41] Bergknut N, Grinwis G, Pickee E, Auriemma E, Lagerstedt AS, Hagman R. et al. Reliability of macroscopic grading of intervertebral disk degeneration in dogs by use of the Thompson system and comparison with low-field magnetic resonance imaging findings. Am J Vet Res 2011;72:899–904.
[42] Bergknut N, Meij BP, Hagman R, de Nies KS, Rutges JP, Smolders LA. et al. Intervertebral disc disease in dogs - part 1: a new histological grading scheme for classification of intervertebral disc degeneration in dogs. Vet J 2013;195:156–63.
[43] Renne C, Willenbrock K, Kuppers R, Hansmann ML, Brauninger A. Autocrine- and paracrine-activated receptor tyrosine kinases in classic Hodgkin lymphoma. Blood 2005;105:4051–9.
[44] Farndale RW, Sayers CA, Barrett AJ. A direct spectrophotometric microassay for sulfated glycosaminoglycans in cartilage cultures. Connect Tissue Res 1982;9:247–8.
[45] Neuman RE, Logan MA. The determination of hydroxyproline. J Biol Chem 1950;184:299–306.
[46] Richardson SM, Purmessur D, Baird P, Probyn B, Freemont AJ, Hoyland JA. Degenerate human nucleus pulposus cells promote neurite outgrowth in neural cells. PLoS One 2012;7:e47735.
[47] Nukaga T, Sakai D, Tanaka M, Hiyama A, Nakai T, Mochida J. Transplantation of activated nucleus pulposus cells after cryopreservation: efficacy study in a canine disc degeneration model. Eur Cell Mater 2016;31:95–106.
[48] Iatridis JC, Nicoll SB, Michalek AJ, Walter BA, Gupta MS. Role of biomechanics in intervertebral disc degeneration and regenerative therapies: what needs repairing in the disc and what are promising biomaterials for its repair? Spine J 2013;13:243–62.
[49] Elliott DM, Yerramalli CS, Beckstein JC, Boxberger JI, Johannessen W, Vresilovic EJ. The effect of relative needle diameter in puncture and sham injection animal models of degeneration. Spine (Phila Pa 1976) 2008;33:588–96.
[50] Carragee EJ, Don AS, Hurwitz EL, Cuellar JM, Carrino JA, Herzog R. 2009 ISSLS prize winner: does discography cause accelerated progression of degeneration changes in the lumbar disc: a ten-year matched cohort study. Spine (Phila Pa 1976) 2009;34:2338–45.
[51] Gruber HE, Rhyne AL 3rd, Hansen KJ, Phillips RC, Hoelscher GL, Ingram JA. et al. Deleterious effects of discography radiocontrast solution on human annulus cell in vitro: changes in cell viability, proliferation, and apoptosis in exposed cells. Spine J 2012;12:329–35.
[52] Chee AV, Ren J, Lenart BA, Chen EY, Zhang Y, An HS. Cytotoxicity of local anesthetics and nonionic contrast agents on bovine intervertebral disc cells cultured in a three-dimensional culture system. Spine J 2014;14:491–8.
[53] Zhang H, Yang S, Wang L, Park P, La Marca F, Hollister SJ. et al. Time course investigation of intervertebral disc degeneration produced by needle-stab injury of the rat caudal spine: laboratory investigation. J Neurosurg Spine 2011;15:404–13.
[54] Nguyen C, Boutron I, Baron G, Sanchez K, Palazzo C, Benchimol R. et al. Intradiscal glucocorticoid injection for patients with chronic low back pain associated with active discopathy: a randomized trial. Ann Intern Med 2017;166:547–56.
[55] Chou R, Atlas SJ, Stanos SP, Rosenquist RW. Nonsurgical interventional therapies for low back pain: a review of the evidence for an American Pain Society clinical practice guideline. Spine (Phila Pa 1976) 2009;34:1078–93.
[56] Datta R, Upadhyay KK. A randomized clinical trial of three different steroid agents for treatment of low backache through the caudal route. Med J Armed Forces India 2011;67:25–33.
[57] Spitzer MS, Mlynczak T, Schultheiss M, Rinker K, Yoeruek E, Petermeier K. et al. Preservative-free triamcinolone acetonide injectable suspension versus "traditional" triamcinolone preparations: impact of aggregate size on retinal biocompatibility. Retina 2011;31:2050–7.
[58] Kropp M, Morawa K-M, Mihov G , Salz A, Harmening N, Franken A. et al. Biocompatibility of poly(ester amide) (PEA) microfibrils in ocular tissues. Polymers 2014;6:243.
[59] Spitzer MS, Kaczmarek RT, Yoeruek E , Petermeier K, Wong D, Heimann H. et al. The distribution, release kinetics, and biocompatibility

of triamcinolone injected and dispersed in silicone oil. Invest Ophthalmol Vis Sci 2009;50:2337–43.
[60] Weinstein RS, Jilka RL, Parfitt AM, Manolagas SC. Inhibition of osteoblastogenesis and promotion of apoptosis of osteoblasts and osteocytes by glucocorticoids. Potential mechanisms of their deleterious effects on bone. J Clin Invest 1998;102:274–82.
[61] Hammond GL. Plasma steroid-binding proteins: primary gatekeepers of steroid hormone action. J Endocrinol 2016;230:R13–25.
[62] Du W, Sun S, Xu Y, Li J, Zhao C, Lan B. et al. The effect of ocular pigmentation on transscleral delivery of triamcinolone acetonide. J Ocul Pharmacol Ther 2013;29:633–8.
[63] Boos N, Weissbach S, Rohrbach H, Weiler C, Spratt KF, Nerlich AG. Classification of age-related changes in lumbar intervertebral discs: 2002 Volvo award in basic science. Spine (Phila Pa 1976) 2002;27:2631–44.
[64] Alini M, Eisenstein SM, Ito K, Little C, Kettler AA, Masuda K. et al. Are animal models useful for studying human disc disorders/degeneration? Eur Spine J 2008;17:2–19.
[65] Eder C, Pinsger A, Schildboeck S, Falkner E, Becker P, Ogon M. Influence of intradiscal medication on nucleus pulposus cells. Spine J 2013;13:1556–62.
[66] Bertolo A, Ettinger L, Aebli N, Haschtmann D, Baur M, Berlemann U. et al. The in vitro effects of dexamethasone, insulin and triiodothyronine on degenerative human intervertebral disc cells under normoxic and hypoxic conditions. Eur Cell Mater 2011;21:221–9.
[67] Khurshid M, Mulet-Sierra A, Adesida A, Sen A. Osteoarthritic human chondrocytes proliferate in 3D co-culture with mesenchymal stem cells in suspension bioreactors. J Tissue Eng Regen Med 2018;12:e1418–32.
[68] Wang JY, Baer AE, Kraus VB, Setton LA. Intervertebral disc cells exhibit differences in gene expression in alginate and monolayer culture. Spine (Phila Pa 1976) 2001;26:1747–51. discussion 1752.
[69] Abe Y, Akeda K, An HS, Aoki Y, Pichika R, Muehleman C. et al. Proinflammatory cytokines stimulate the expression of nerve growth factor by human intervertebral disc cells. Spine (Phila Pa 1976) 2007;32:635–42.
[70] Marshall LL, Trethewie ER, Curtain CC. Chemical radiculitis. A clinical, physiological and immunological study. Clin Orthop Relat Res 1977;129:61–7.
[71] Takahashi H, Suguro T, Okazima Y, Motegi M, Okada Y, Kakiuchi T. Inflammatory cytokines in the herniated disc of the lumbar spine. Spine (Phila Pa 1976) 1996;21:218–24.
[72] Muramoto T, Atsuta Y, Iwahara T, Sato M, Takemitsu Y. The action of prostaglandin E2 and triamcinolone acetonide on the firing activity of lumbar nerve roots. Int Orthop 1997;21:172–5.
[73] Kim SW, Im YJ, Choi HC, Kang HJ, Kim JY, Kim JH. Urinary nerve growth factor correlates with the severity of urgency and pain. Int Urogynecol J 2014;25:1561–7.
[74] Liu HT, Tyagi P, Chancellor MB, Kuo HC. Urinary nerve growth factor but not prostaglandin E2 increases in patients with interstitial cystitis/bladder pain syndrome and detrusor overactivity. BJU Int 2010;106:1681–5.
[75] Reed BD, Plegue MA, Sen A, Haefner HK, Siddiqui J, Remick DG. Nerve growth factor and selected cytokines in women with and without vulvodynia. J Low Genit Tract Dis 2018;22:139–46.
[76] Jayabalan P, Schnitzer TJ. Tanezumab in the treatment of chronic musculoskeletal conditions. Expert Opin Biol Ther 2017;17:245–54.
[77] Li X, Zhang Y, Song B, En H, Gao S, Zhang S. et al. Experimental application of bone marrow mesenchymal stem cells for the repair of intervertebral disc annulus fibrosus. Med Sci Monit 2016;22:4426–30.